

DOE/CE/23810-82

INFRARED ANALYSIS OF REFRIGERANT MIXTURES

Final Report
January 24, 1998

T.F. Morse

Hope Technologies, Corp.
22 Benevolent St.
Providence, RI 02906

Prepared for
The Air-Conditioning and Refrigeration Technology Institute
under
ARTI MCLR Project Number 660-54000

This project is supported in part, by US Department of Energy (Office of Building Technology) grant number GEF02-91C2381Q: Material Compatibility and Lubricant Research (MCLR) on CFC-Refrigerant substitutes. Federal funding supporting this project constitutes 93.57% of allowable costs. Funding from non-government sources supporting this project consists of direct cost sharing of 6.43% of allowable costs, and in-kind contributions from the air-condition and refrigeration industry.

Prepared for the Air-Conditioning and Refrigeration Technology Institute
under
ARTI MCLR Research 660-5400: Infrared Analysis of Refrigerant Mixtures,
DOE/CE/23810-82

This project is supported, in whole or in part, by US. Department of Energy grant number DE-FG02CE2381: Materials Compatibility and Lubricant Research (MCLR) on CFC-Refrigerant Substitutes. Federal funding supporting this project constitutes 93.57% of allowable costs. Funding from non-government sources supporting this project consists of direct cost sharing of 6.43% of allowable costs; and the in-kind contributions from the air-conditioning and refrigeration industry.

DISCLAIMER

The U.S. Department of Energy and the air-conditioning and refrigeration industry's support for the Materials Compatibility and Lubricants Research (MCLR) program does not constitute an endorsement by the U.S. Department of Energy, nor by the air-conditioning industry, of the views expressed herein.

NOTICE

This study was sponsored by the United States Government. Neither the United States Government, nor the Department of Energy, nor the Air-Conditioning and Refrigeration Technology Institute (ARTI), nor any of their employees, nor any of their contractors nor subcontractors make any warranty, expressed or implied, or assume any legal liability or responsibility for the accuracy, completeness, or usefulness of any information, apparatus, product, or process disclosed or represents that its use would not infringe privately-owned rights.

COPYRIGHT NOTICE

(for journal publications submissions)

By acceptance of this article, the publisher and/or recipient acknowledge the rights of the U.S. Government and the Air-Conditioning and Refrigeration Technology Institutes, Inc. to retain a non-exclusive, royalty-free license in and to any copyrights covering this paper.

Abstract

In order to assess the viability of using the concept of intra-cavity laser spectroscopy as a tool for the identification of newly approved refrigerant gases, we have performed a series of experiments on the infrared absorption characteristics of a series of these gases. In particular, we have obtained values for the absorption of these gases in the 1.65-2.0 micron range. This is of particular interest when applying the principle of FLICS (Fiber Laser Intra-Cavity Spectroscopy) in conjunction with the broad gain bandwidth of the Tm (thulium) fiber laser. In order to clarify how this concept can be carried out with regard to refrigerant gases, we have performed some model preliminary experiments using acetylene as a test gas. This was done to establish the principle of this new sensing technique.

Table of Contents

Abstract	iii.
List of Figures	v.
I. Introduction	1.
II. Fiber Laser Intra-Cavity Spectroscopy (FLICS)	1.
III. Measurements of Infrared absorption of refrigerant gases	3.
A. R-12 and R-115	3.
B. R-22 and R-124	3.
C. R-134a, R-32, R-125, R-152a	3.
D. Refrigerant Mixtures	4.
R-22 and R-407c	4.
R-12 and R-401a	4.
R-502 and R-404a	5.
IV. Conclusions	5.

List of Figures

- Figure 1. Traditional Absorption Spectroscopy
- Figure 2. Schematic of FLICS
- Figure 3. Lasing line in FLICS device with no acetylene in cavity
- Figure 4. Acetylene placed in absorption cell, laser line tuned off acetylene absorption
- Figure 5. Compression tuning of fiber Bragg grating
- Figure 6. Fiber grating tuned to acetylene line
- Figure 7. Absorption of R-12
- Figure 8. Absorption of R-115
- Figure 9. Absorption of R-22
- Figure 10. Absorption of R-124
- Figure 11. Absorption of R-134a
- Figure 12. Absorption of R-32
- Figure 13. Absorption of R-125
- Figure 14. Absorption of R-152a
- Figure 15. Absorption of 100% R-502
- Figure 16. Absorption of R-404A
- Figure 17. Absorption of 10% R-404A and 90% R-502
- Figure 18. Absorption of 50% R-404A and 50% R-502
- Figure 19. Absorption of 90% R-404A and 10% R-502
- Figure 20. Absorption of different percentages of R-404A and R-502

I. Introduction

New classes of refrigerant gases have come into being as a consequence recent modifications in environmental restrictions. This has, in part, occurred to make refrigerant gases environmentally "friendly" with respect to their influence on the ozone layer. It is of importance to be able to detect the presence of these new gases as well as older gases to determine if systems are functioning properly. Other reasons that create a demand for quantitative measurements of the presence of such gases are: leak detection during the manufacturing stage of air conditioning elements to determine if they are leak free, or for the determination of mixture ratios in newer systems to learn if they are operating at maximum efficiency with proper mixture ratios.

For these reasons, a more convenient, and inexpensive gas sensor would be of use. These measurements can be made with Fourier Transform Spectroscopy; however, these instruments are unwieldy and expensive. Further, it is desired that it not be necessary for a trained technician to operate and maintain the equipment, and it should be a device that can readily be operated under field conditions. To this end, we have proposed a new type of gas sensor, FLICS (Fiber Laser Intra-Cavity Spectroscopy) that holds reasonable promise of fulfilling this function. Further research and development are needed to carry this principle to a useful conclusion.

II. Fiber Laser Intra-Cavity Spectroscopy (FLICS)

It is well known that when radiation passes through an absorbing medium, the radiation intensity diminishes exponentially. This type of spectroscopy is schematically illustrated in [Figure 1](#). However, if an absorber is placed within the laser cavity, the gain is "spoiled", and there can be an enormous increase in the sensitivity of detection as a consequence of high reflectivity output coupling mirrors that cause the photons to pass back and forth many times through the absorber before exiting. In addition, for situations in which the laser linewidth is broader than the linewidth of the absorber within the cavity, a complex modal interaction provides further enhanced sensitivity to the presence of the absorber. In [Figure 2](#), we see how this principle can be applied to the detection of a gas (or liquid) that has an absorption signature within the gain bandwidth of the optical fiber laser. The device, in principle, is quite

simple, consisting of an optical fiber laser with a Bragg mirror grating, a collimating lens, an open section in which the absorber can be placed, a high reflectivity mirror so that the laser cavity is defined as that space between the Bragg grating mirror and the 100% reflective mirror. Ordinary fiber is used to carry the pump light from an optical diode and, through a 2 x 2 coupler, to a detector. It is evident that this configuration could be developed further to be completely portable, relatively inexpensive, and compact.

In order to demonstrate how the presence of a gas can be detected using this concept, we consider the use of acetylene as a model gas. This was chosen because our present capability in the fabrication of Bragg gratings is limited to those wavelengths at which we have a proper phase mask to illuminate with excimer radiation. We are in the process of acquiring a FRED (Frequency Doubled) argon ion laser which will provide intra cavity doubling of the 488 nm line of argon to obtain 244 nm radiation that can be used to "write" gratings in a germanium, hydrogen loaded optical fiber. At the present time, our phase masks are at 1,535 nm and this corresponds to the absorption wavelength of acetylene. In [Figure 3](#) we see the strong lasing signal at 1538 nm from a FLICS device with no gas in the absorption cell. If 1 atm. of acetylene is placed in the absorption cell, and if the laser is tuned between the absorption lines of the acetylene gas in the cell, we then obtain the lasing signal shown in [Figure 4](#). The fluorescence from the side bands of the laser make the acetylene lines visible in the shoulder of the laser line. In order for such a device to function as a gas sensor, it is necessary to be able to tune such a device. We have developed several techniques in order to be able to accomplish this. The optical fiber Bragg grating can be attached to a thin sheet of plastic, and the plastic bent so that the optical fiber is compressed. With this technique we have been able to tune the Bragg grating over 19 nm. This is illustrated in [Figure 5](#). More recent experiments have demonstrated that using a HOCC (High OverCoupled Coupler) as the output mirror on an erbium ring fiber laser, it has been possible to tune 43 nm over the erbium fiber gain bandwidth. If the peak reflectivity of the Bragg grating is now detuned by as little as .1 nm, so that the fiber laser wavelength corresponds to an absorption peak of the acetylene, we see that there is a decrease of five orders a magnitude of intensity in the laser line. This is shown in [Figure 6](#). It is this reduction of signal that denotes the presence of an absorber at the specific acetylene

line, and it is this principle upon which our refrigerant gas detection system would be based.

With this concept in mind as background, we are able to consider its application to the convenient detection of refrigerant gases, and mixtures of refrigerant gases.

III. Measurements of Infrared absorption of refrigerant gases

Measurements were performed by Prof. Risen in Chemistry on a Nicolet monochromator. Various pressures were used, but it was determined that a gas pressure of 500 Torr and an absorption path length of 20 cm were appropriate. In order to use the above procedure to detect gases of interest, it is necessary that there be absorption under the gain bandwidth of the optical fiber laser. For the case of Tm, this is in the 1,660-1,900 nm regime, so that our interest will focus on the strongest absorption lines in this wavelength region.

A. R-12 and R-115

First we consider the absorption spectra of R-12 and R-115. These are shown in [Figures 7](#) and [8](#). It is seen that there are no distinguishing characteristics in the wavelength range 900-2,400 nm. All of the newer refrigerant compounds have absorption signatures in the 1,680-1,950 nm region. Thus, if a gas is used as a refrigerant gas and it has no absorption in this wavelength region, it clearly is, at best, a mixture of the older type of refrigerant. This in itself provides possible useful information toward the classification of the type of refrigerant gas.

B. R-22 and R-124

We now consider R-22 and R-124. In [Figure 9](#) is depicted the absorption of R-22. It can be seen that there is a strong absorption line at 1,687.2 nm, and a reasonably strong line at 1,789 nm. These provide a good "fingerprint" accessible to the Tm fiber laser. In [Figure 10](#) is shown the absorption spectrum of R-124. A strong absorption line is present at 1,698 nm.

C. R-134a, R-32, R-125, R-152a

No measurements were made on R-143A as we did not receive any sample of this gas. In [Figure 11](#) we show the infrared spectrum of R-134a. For detection purposes, there is a reasonably strong line

of R-134a. For detection purposes, there is a reasonably strong line at 1,724.3 nm. Figure 12 depicts the spectrum for R-32. There is a line at 1,725 of moderate strength. It is believed that the detection scheme proposed above could detect this. The moderate absorption line strength of R-125 at 1,713.6 nm is shown in Figure 13. In Figure 14, the corresponding spectrum for R-152a with a weaker absorption line at 1,707 nm is shown. These results are summarized in the following table.

refrigerant	wavelength	absorption	wavelength	absorption
R-22	1687 nm	strong	1789 nm	medium
R-32	1661 nm	weak	1725 nm	weak
R-124	1698 nm	strong	1744 nm	weak
R-125	1689 nm	medium	1715 nm	medium
R-134a	1666 nm	medium	1724 nm	medium
R-152a	1707 nm	weak	1775 nm	weak

Table 1: Summary of Refrigerant Absorption in the 1660-1790 nm regime

Thus, in order of ease of detection, first come R-22 and R-124, then R-125 and R-134a, and finally, the weaker lines of R-32 and R-152a.

D. Refrigerant Mixtures

In the following, we wish to consider mixtures of refrigerant replacements. We did not receive the R-407C and R-401A mixtures, however, it is possible to comment on what would occur in mixtures of R-22 and R-407C as well as mixtures of R-12 and R-401A.

R-22 and R-407C

In this case, we note that 407C consists of 23% R-32, 25% R-125, and 52% R134a. There is a strong line of R-22 at 1687 nm, and a medium line in the 407c (from R-125) at 1689 nm. A ratio of the intensity of these two lines could be used to obtain information on relative content.

R-12 and R401A

For a mixture of R-12 and R-401A, we note that there is no absorption in the wavelength region under consideration here;

however, there is a strong absorption in the R-401a (caused by 52% R-22) at 1687 nm as well as at 1698 nm (caused by 34% R-124).

R-502 and R-404a

In these mixtures, we have in R-502: R-22 (48%), and R-115 (52%). In R-404A we have: R-125 (44%), R-143a (52%) and R-134a (4%). The R-143a (4%) material was not received and therefore not evaluated. Consequently, in the R-502 the strongest absorption signature comes from R-22, and from R-404a, the strongest absorption signature comes from the medium strength lines of R-125 and R-134a.

In figures 15 and 16 are shown 100% R-502 and R-404a, respectively. Figure 17 has 10% R-404a and 90% R-502; Figure 18 shows 50% each of R-404a and R-502. Figure 19 shows 90% of R-404a and 10% R-502. In Figure 20, all of these mixtures are presented together. It can be seen that there is sufficient spectroscopic signal to differentiate between the relative amounts of each of these gas mixtures in the wavelength region accessible to the Tm fiber laser.

IV. Conclusions

Measurements of a series of refrigerant gases has been measured with particular emphasis on the spectroscopic signature of those gases in the near IR. In particular, we have described how the techniques of FLICS (Fiber Laser Intra Cavity Spectroscopy) may be used to detect the presence of an absorber under the gain bandwidth of the fiber laser. We have demonstrated the use of this technique employing acetylene as a test gas. With the Tm fiber laser, with a gain bandwidth from 1650 to 2090 microns, we believe that there are a host of the constituents of new refrigerant gases that can be quantitatively detected using the principles described above. Further work will be needed to demonstrate the detectability of these compounds using a Tm fiber laser, but it is believed that detection can be achieved to within a few percent for the gases discussed above.

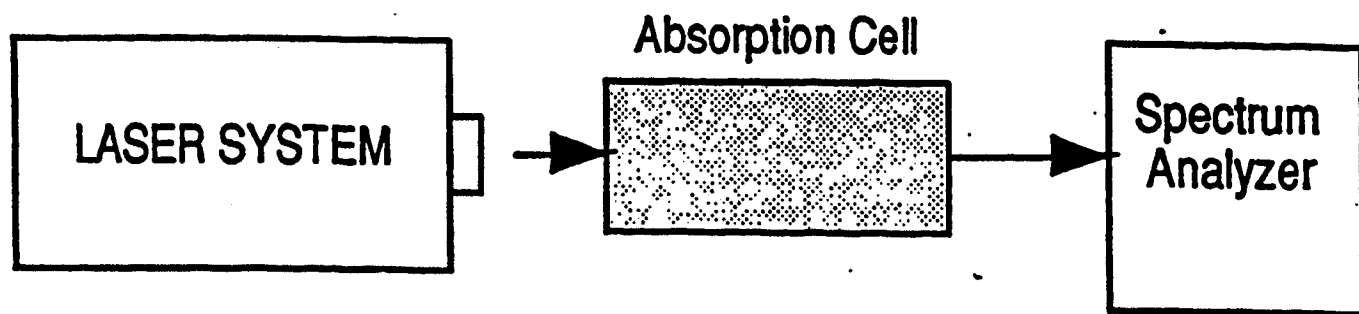


Figure 1. Traditional Absorption Spectroscopy

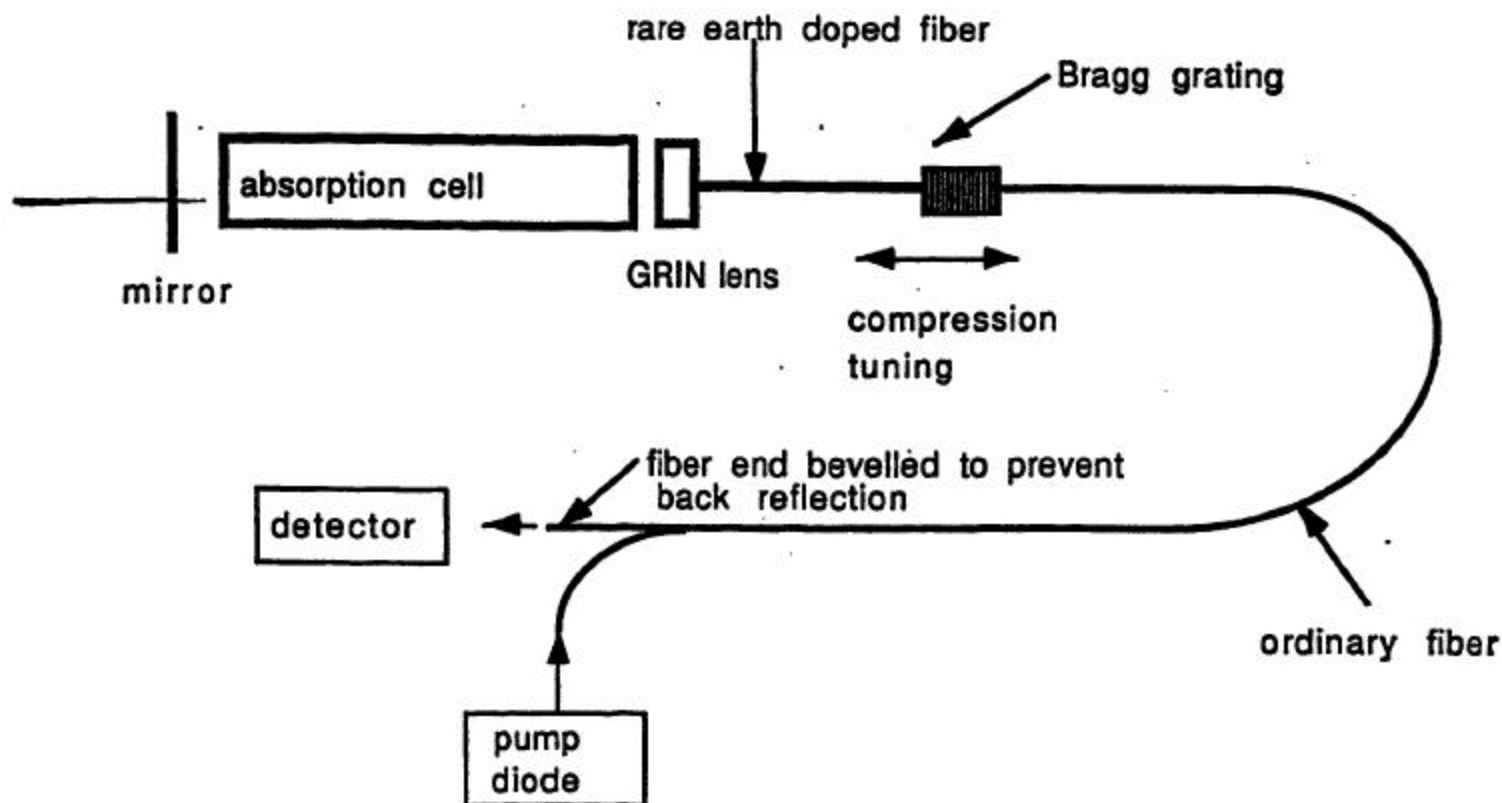


Figure 2. Schematic of FLICS

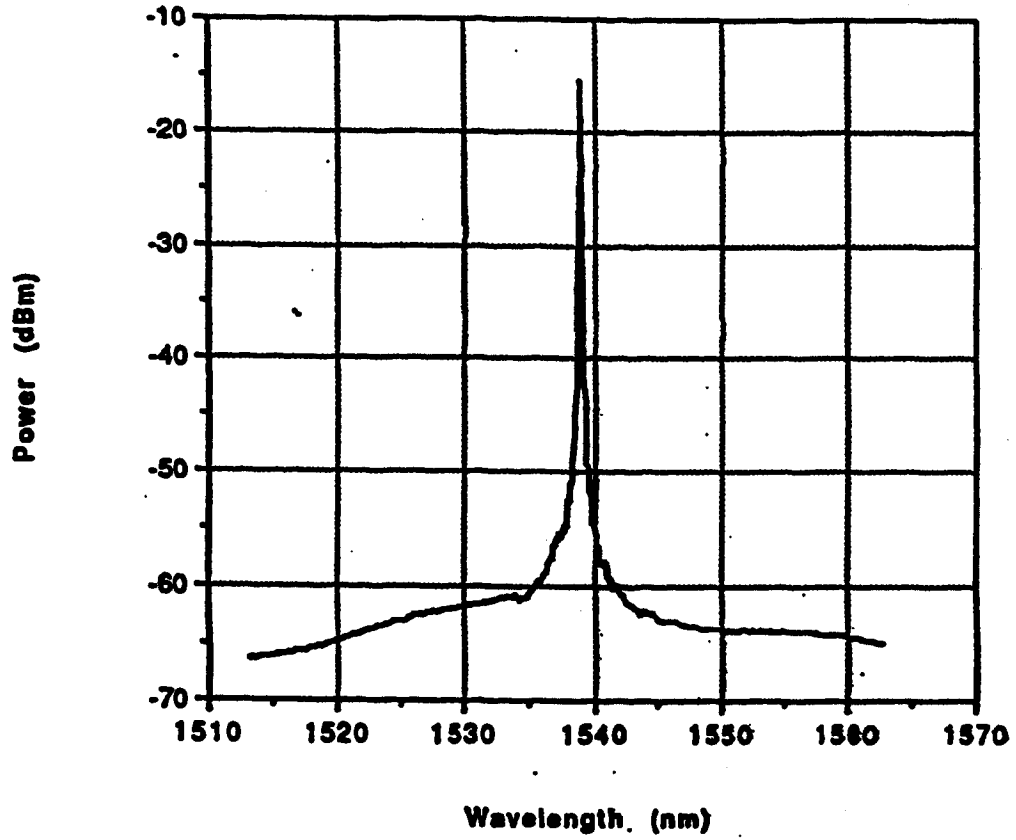


Figure 3. Lasing line in FLICS device with no acetylene in cavity

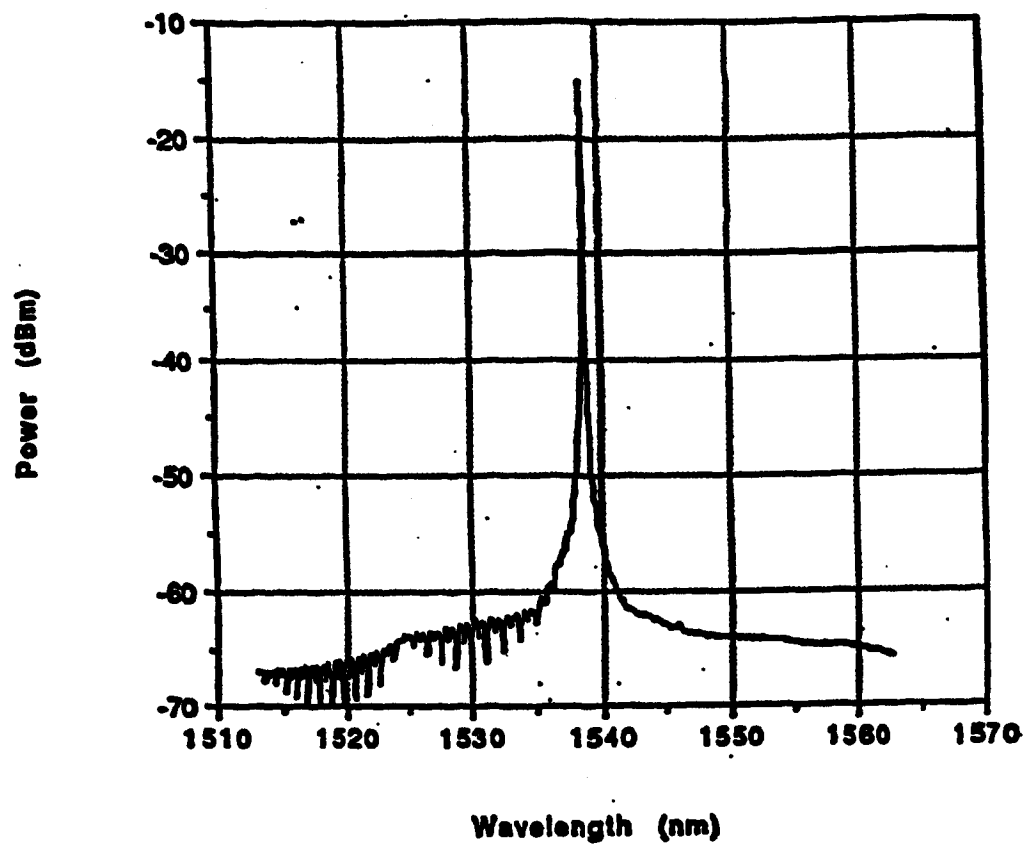


Figure 4. Acetylene placed in absorption cell, laser line tuned off acetylene absorption

Two Point Bending

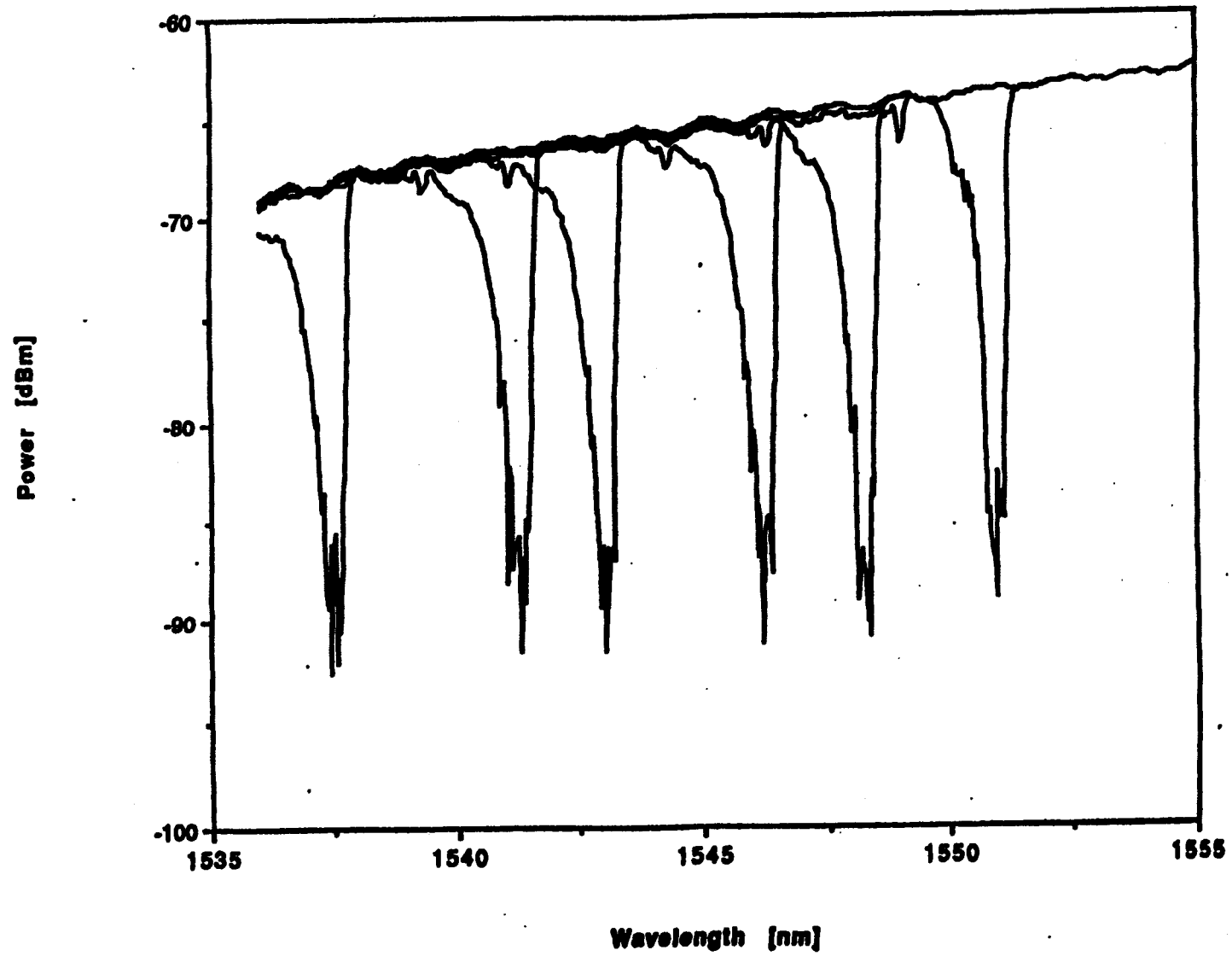


Figure 5. Compression tuning of fiber Bragg grating

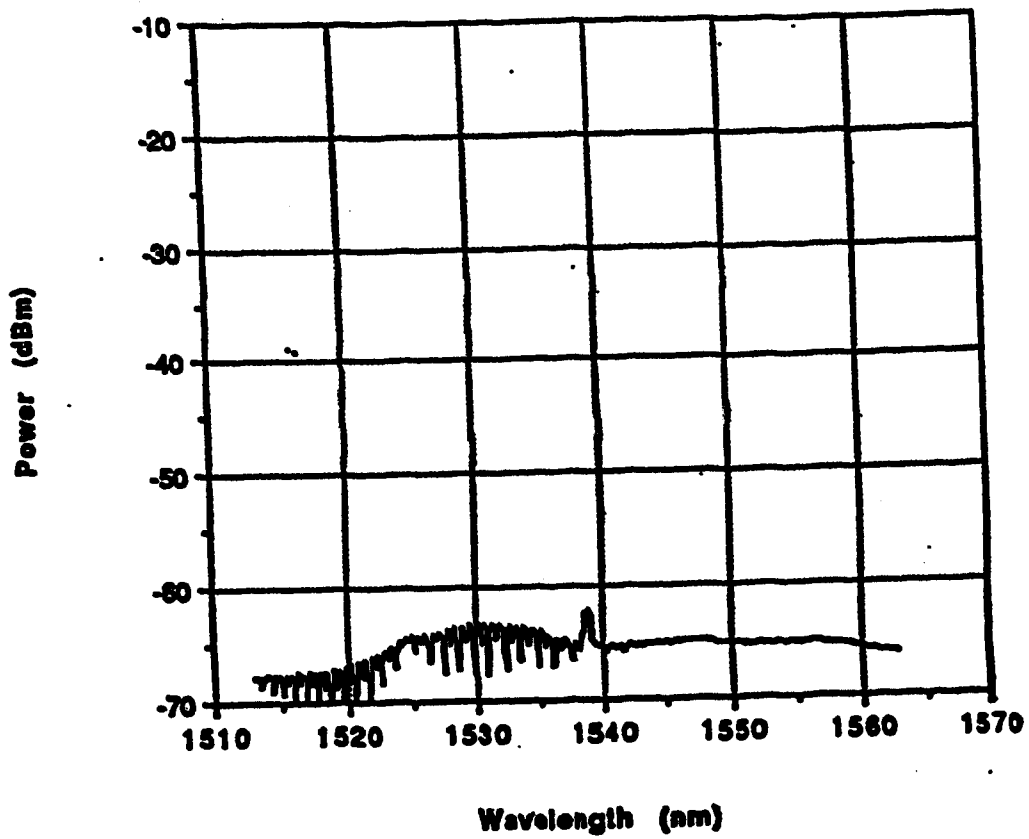


Figure 6. Fiber grating tuned to acetylene line

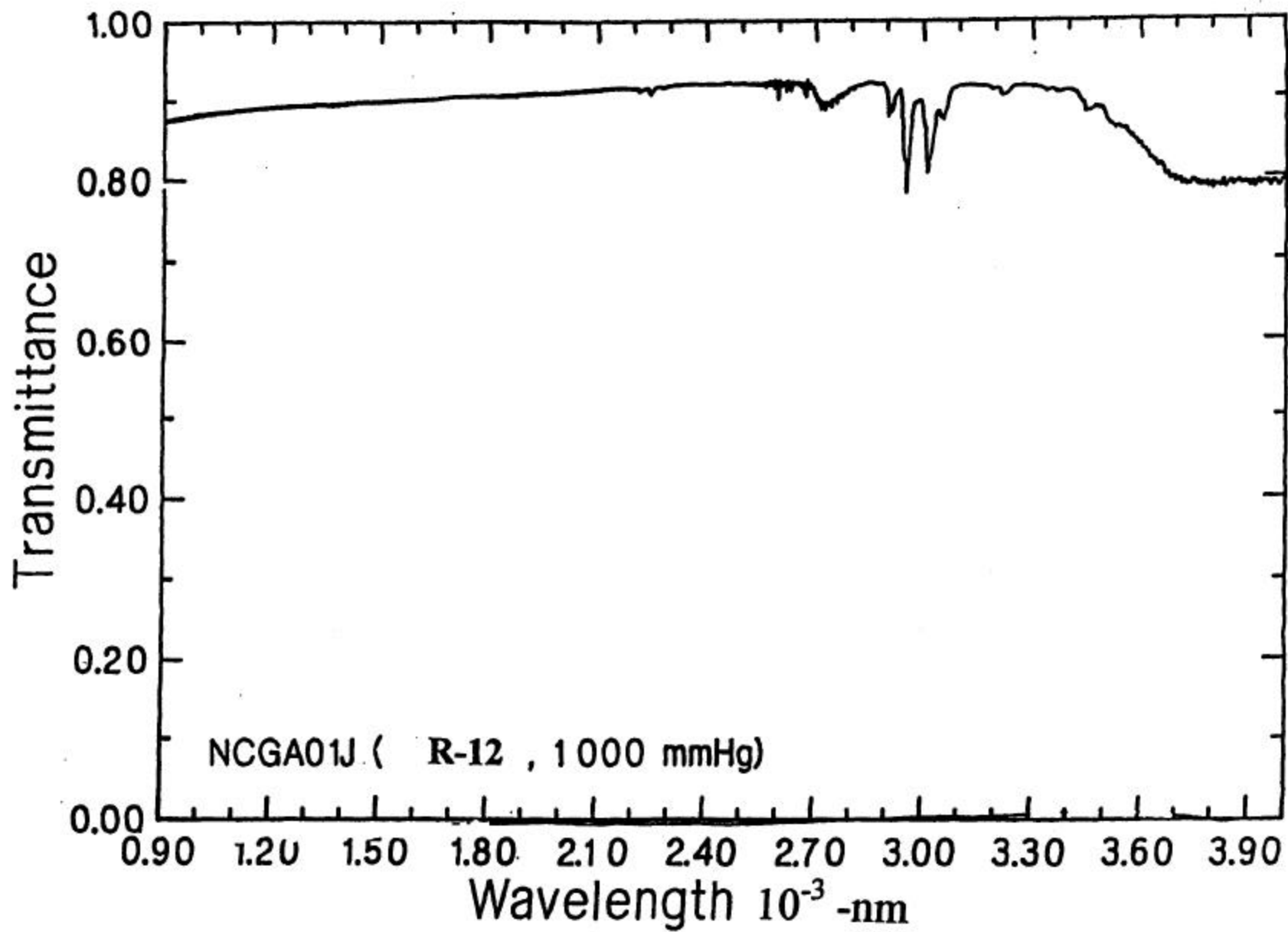


Figure 7. Absorption of R-12

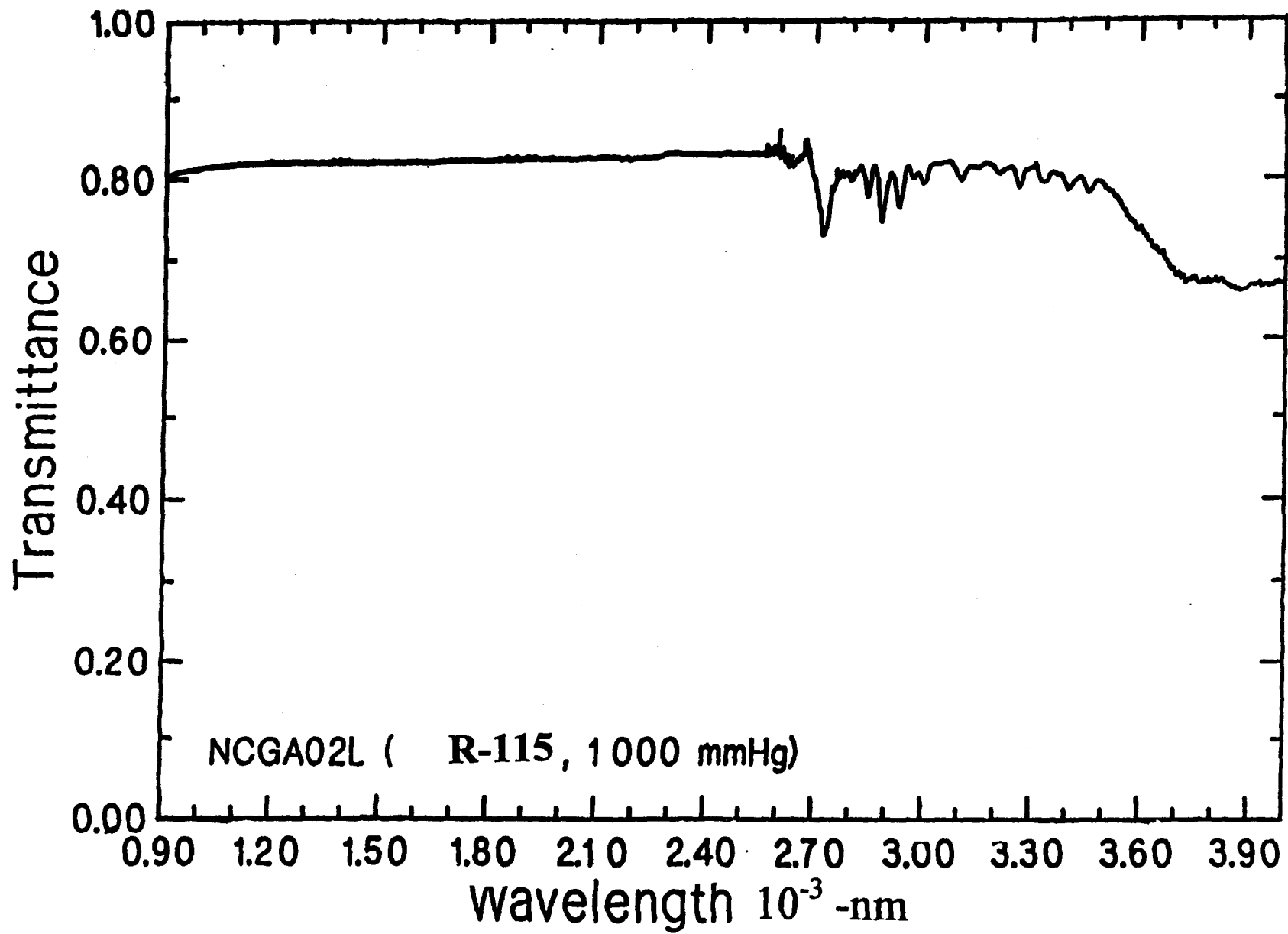


Figure 8. Absorption of R-115

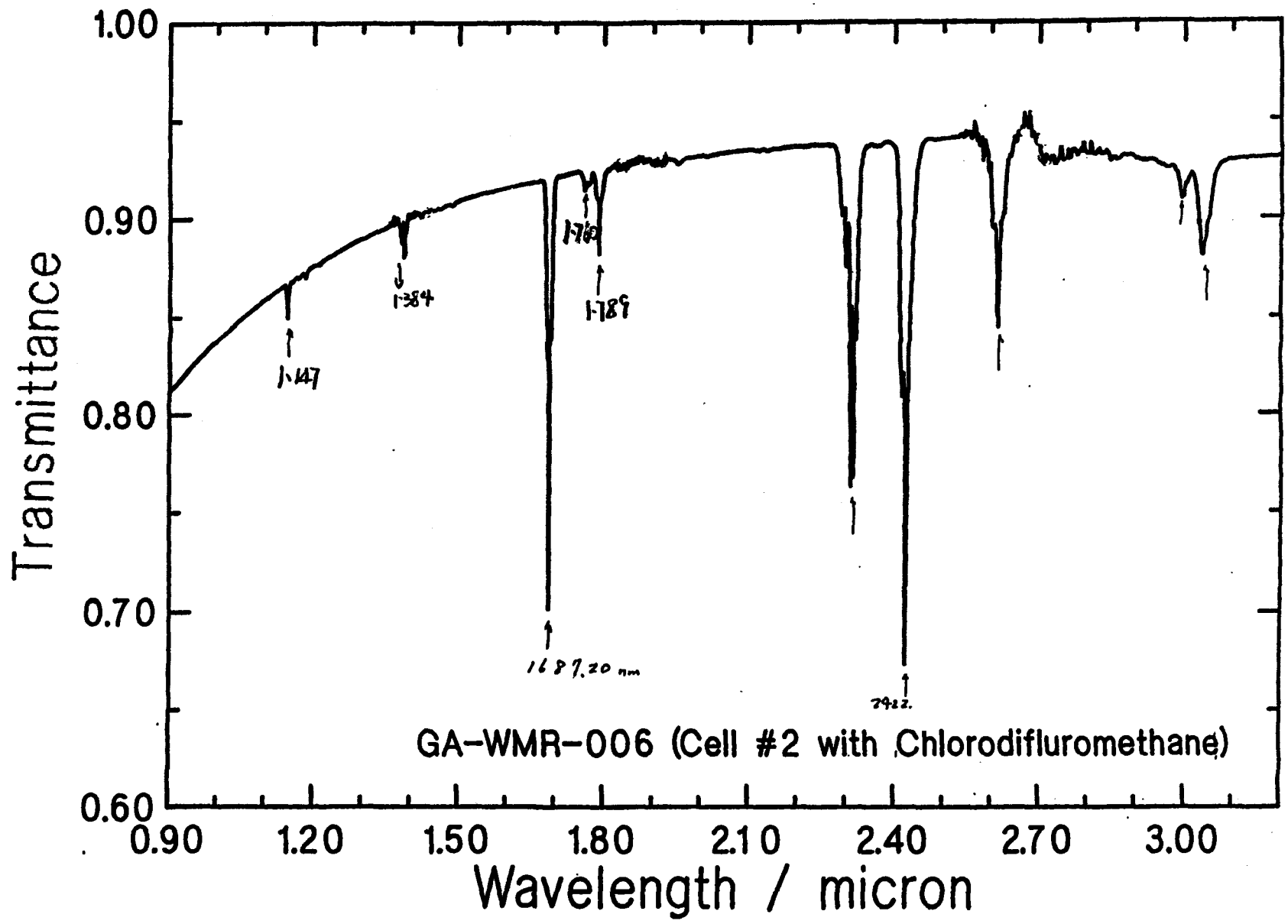


Figure 9. Absorption of R-22

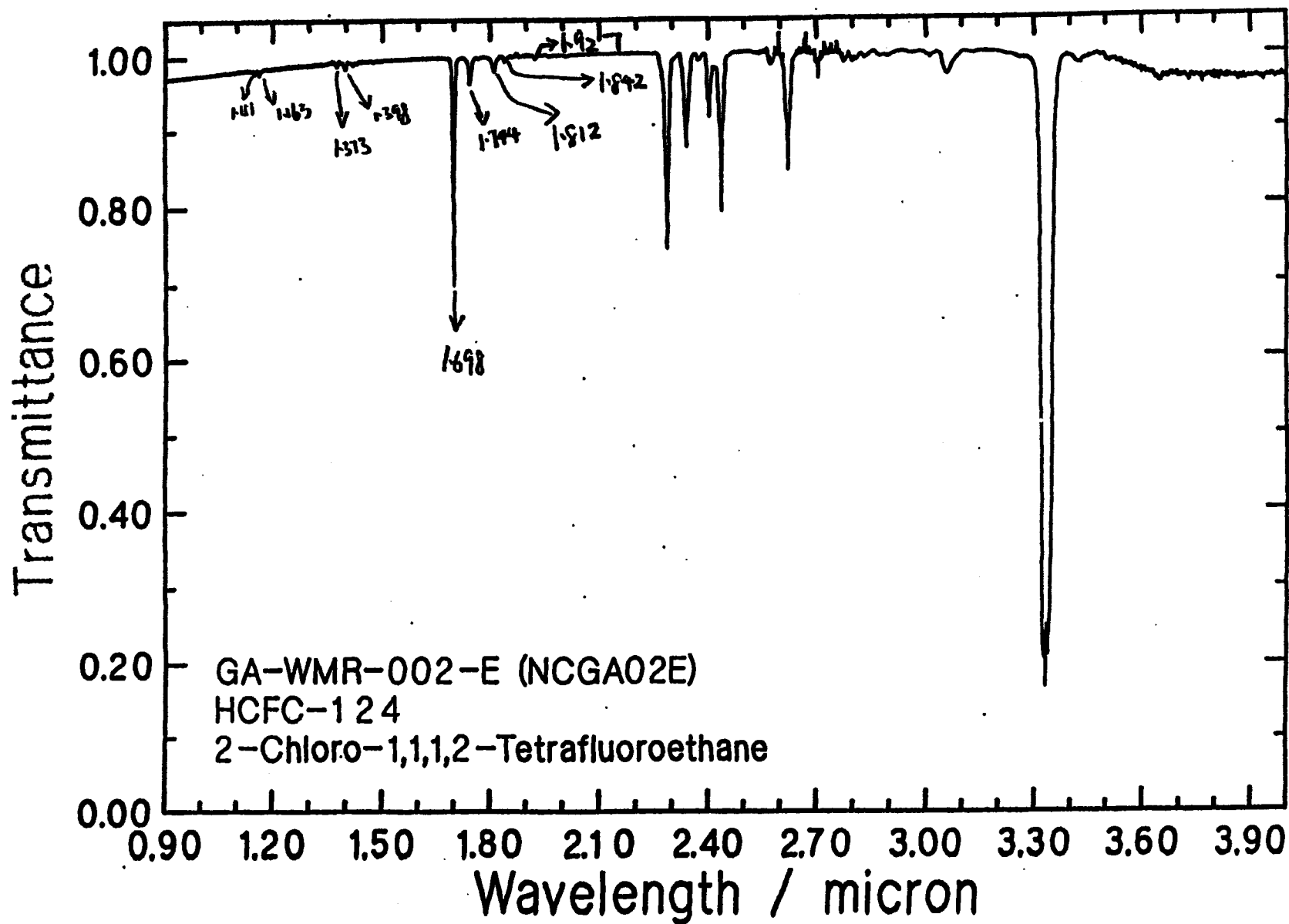


Figure 10. Absorption of R-124

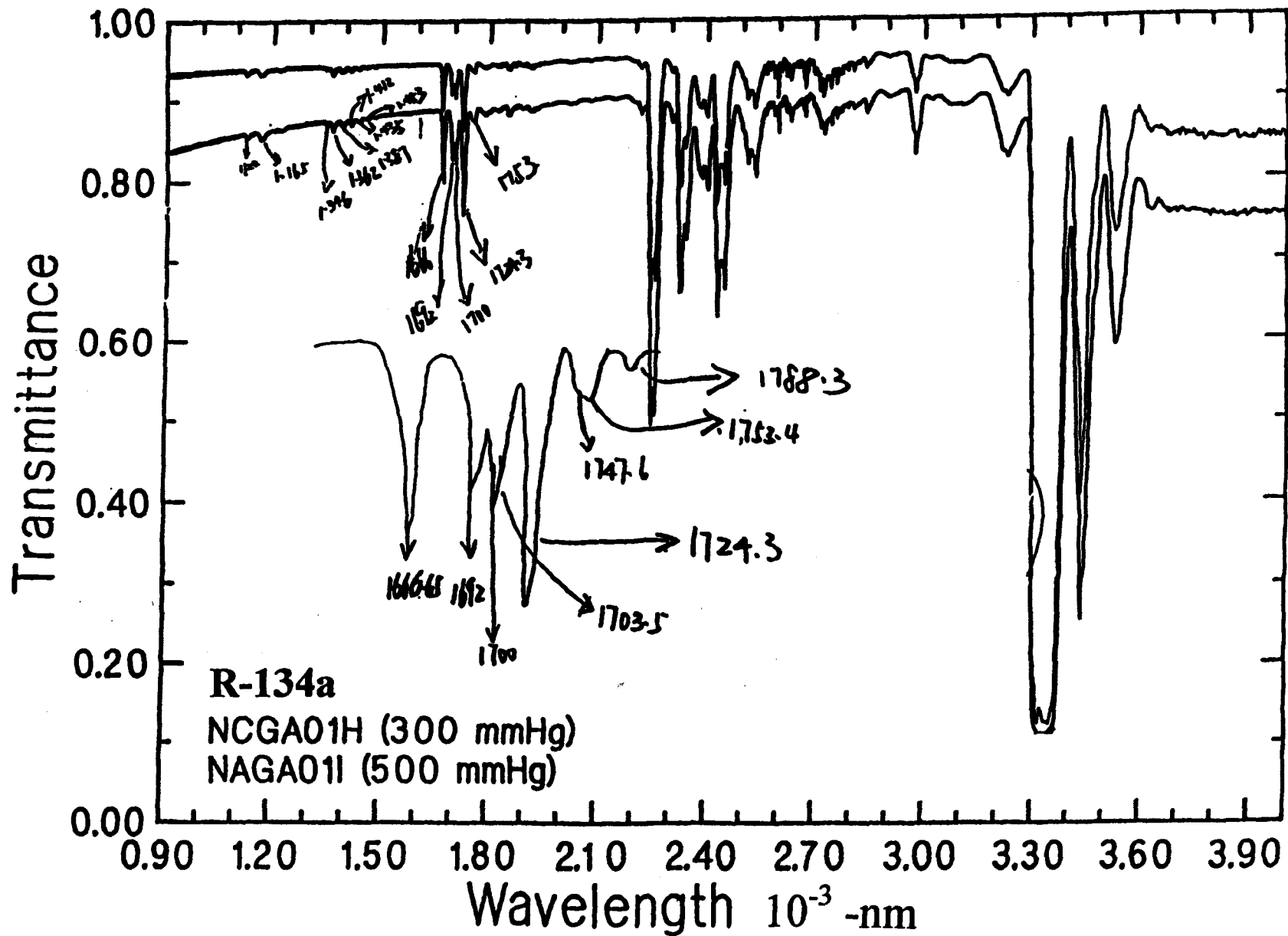


Figure 11. Absorption of R-134a

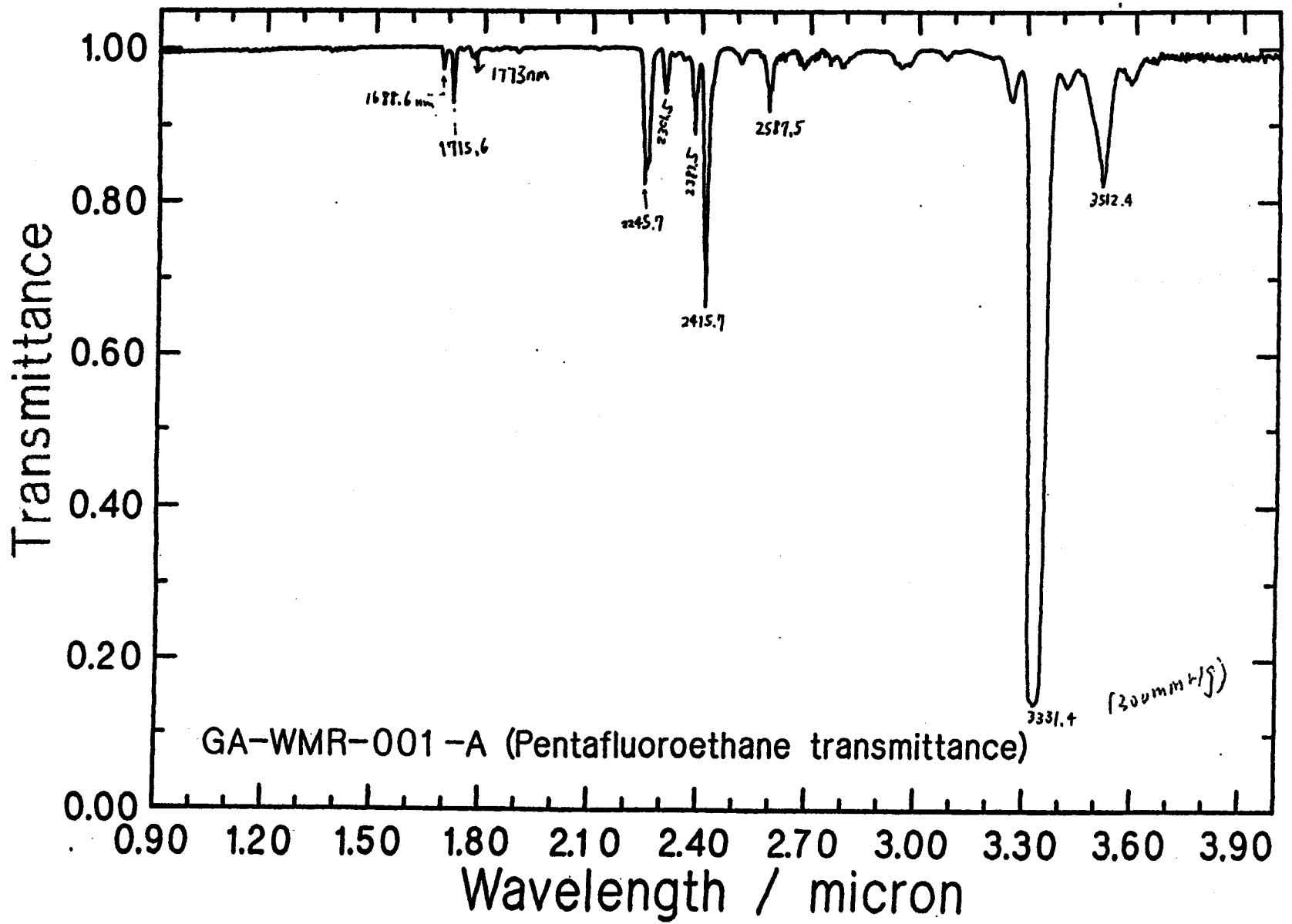


Figure 13. Absorption of R-125

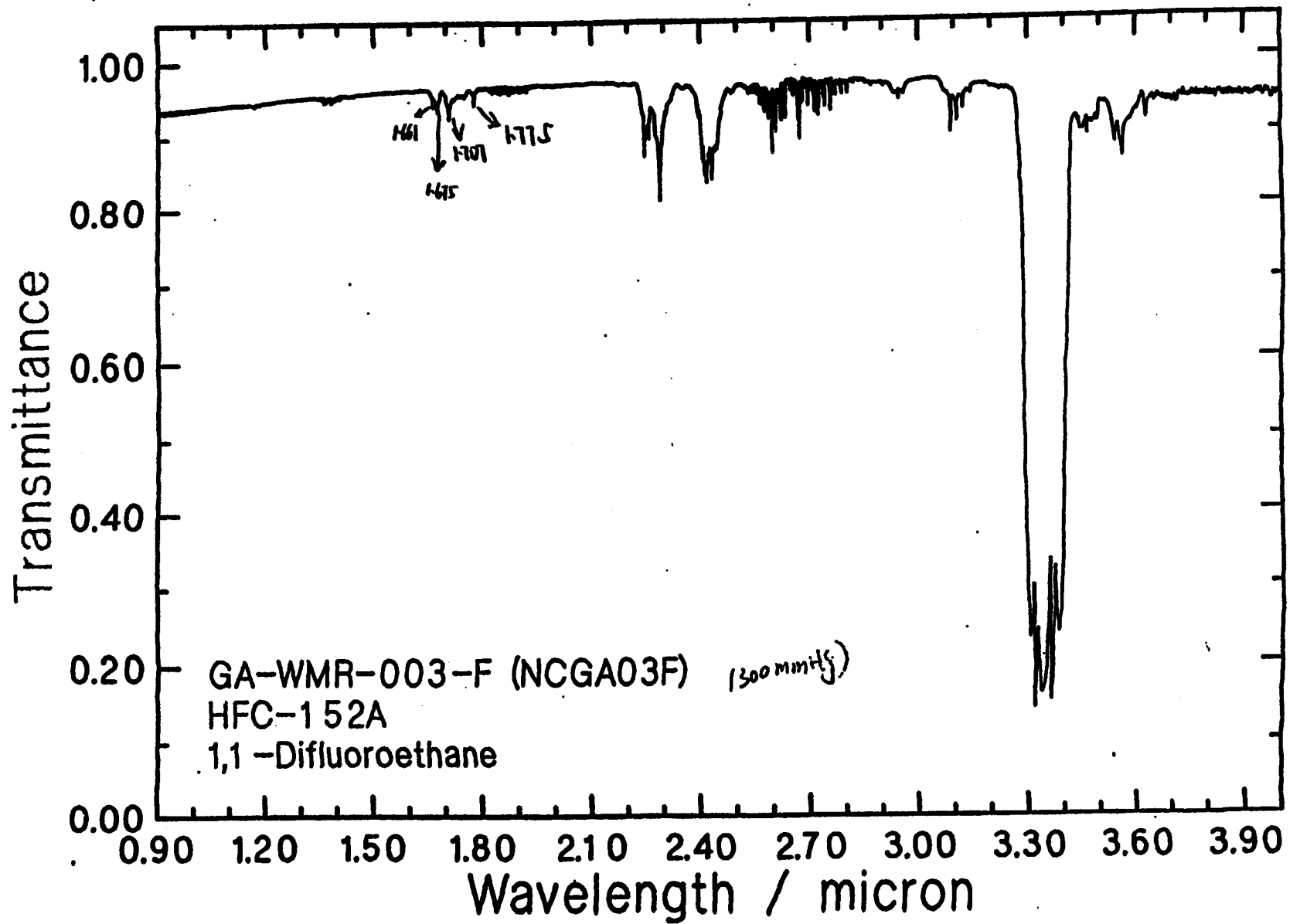


Figure 14. Absorption of R-152a

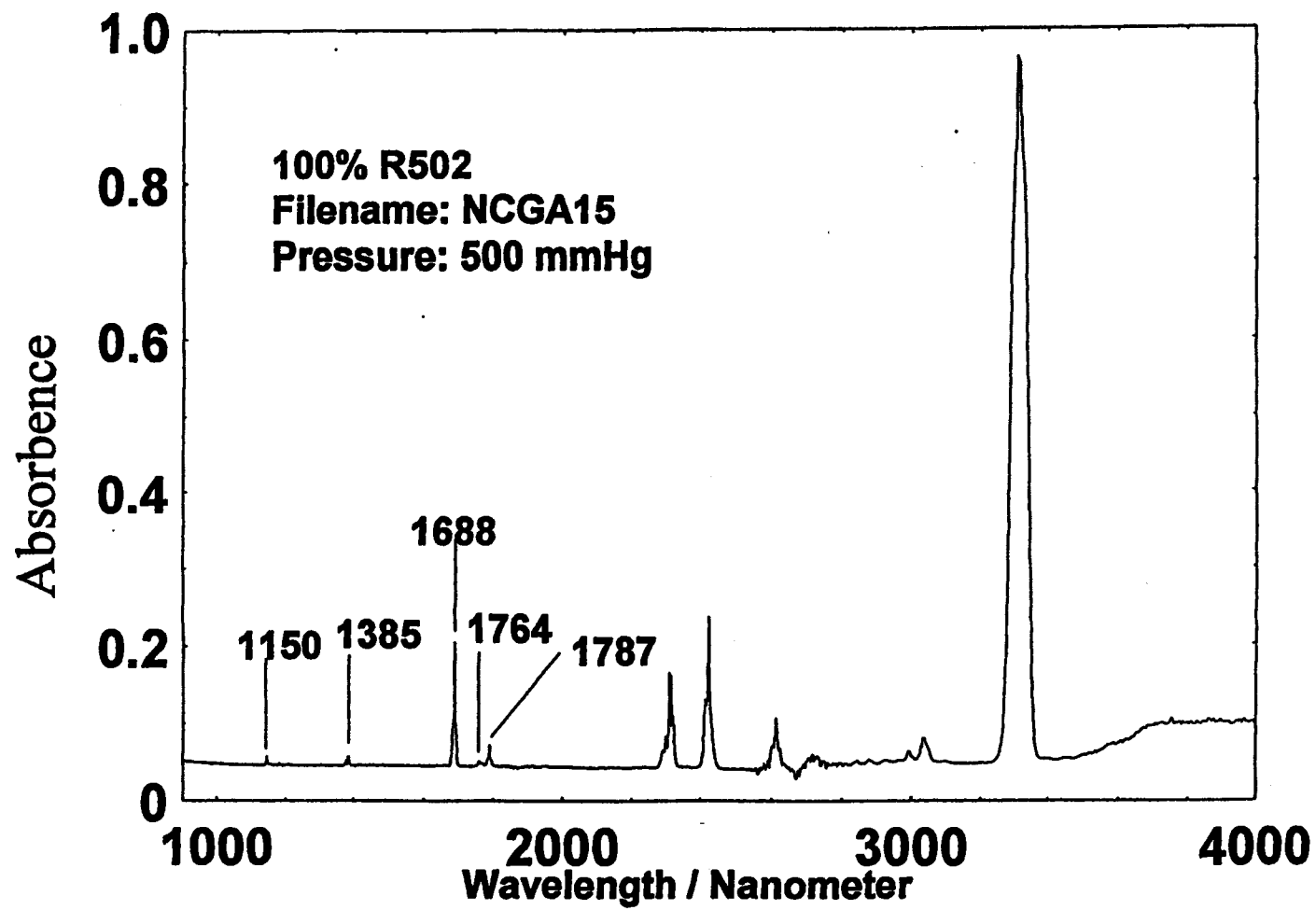


Figure 15. Absorption of 100% R-502

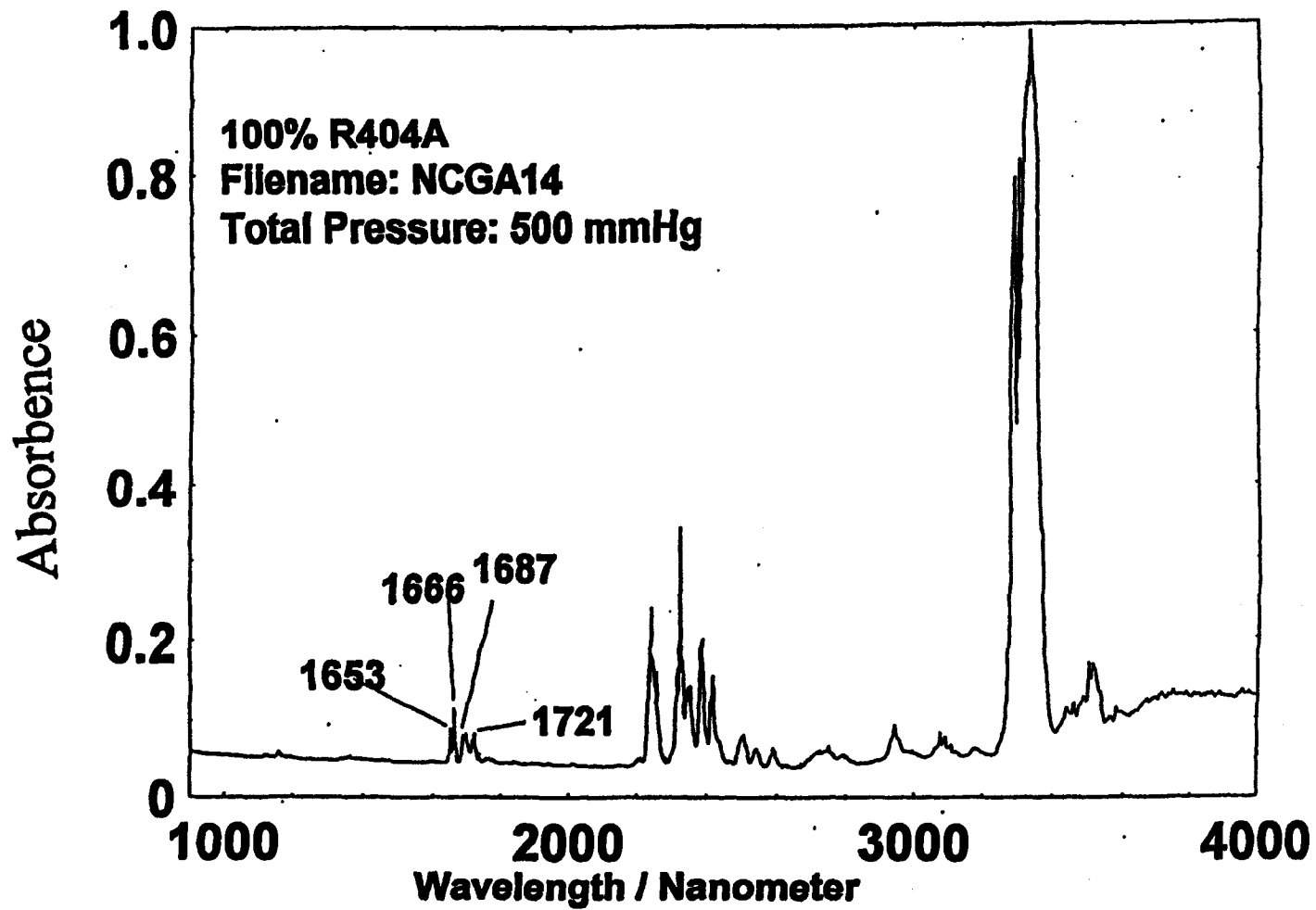


Figure 16. Absorption of 100% R-404A

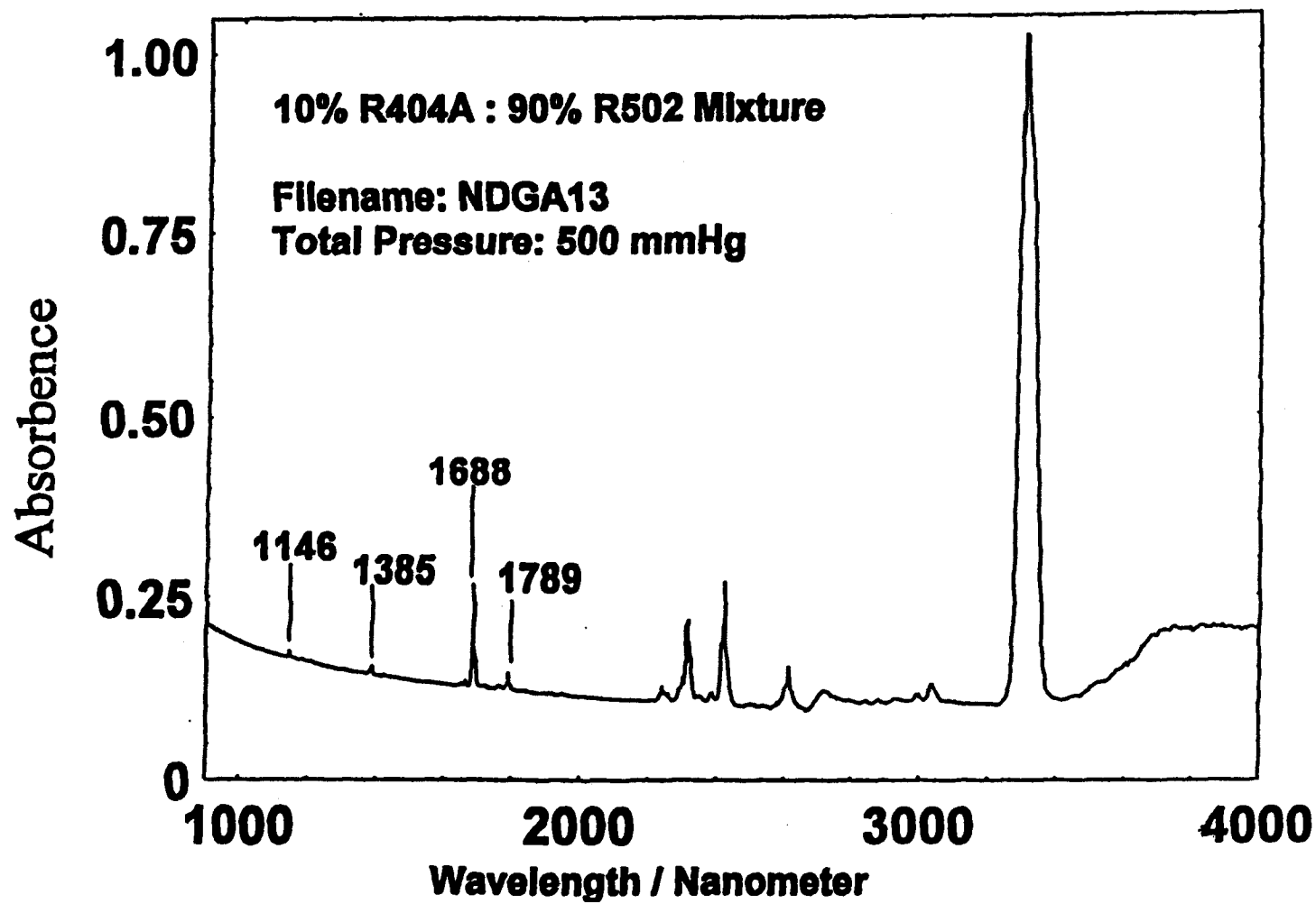


Figure 17. Absorption of 10% R-404A and 90% R-502

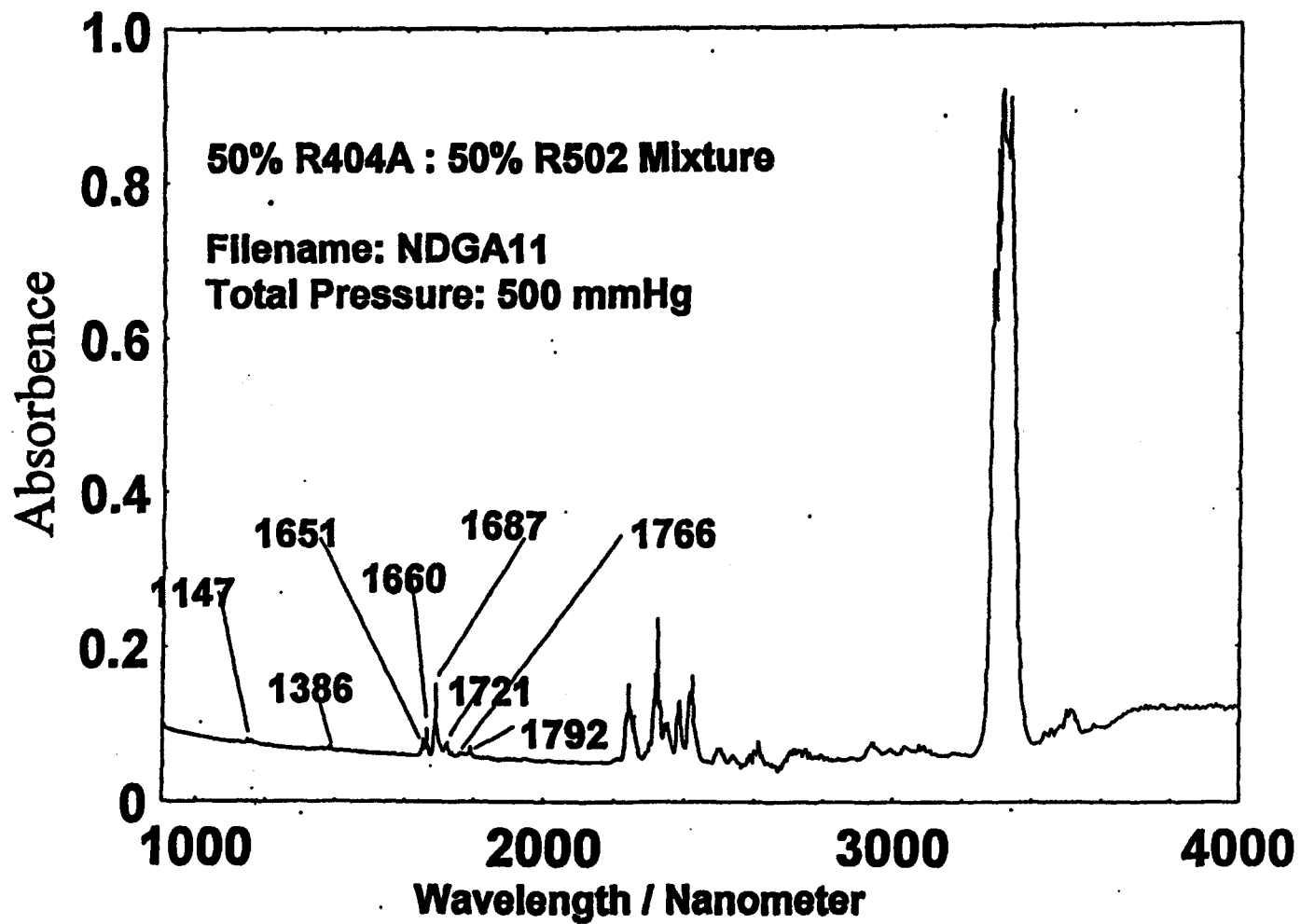


Figure 18. Absorption of 50% R-404A and 50% R-502

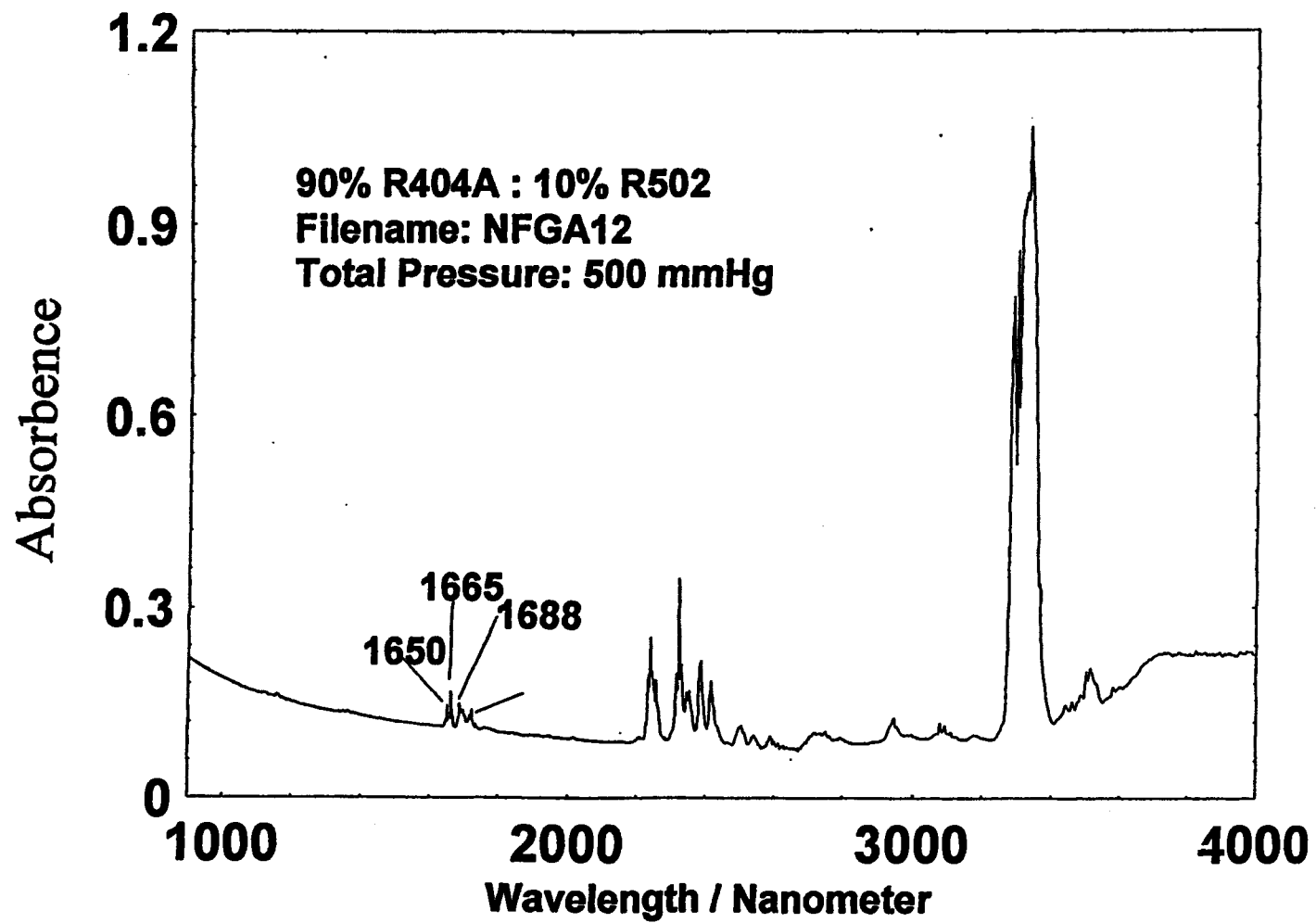


Figure 19. Absorption of 90% R-404A and 10% R-502

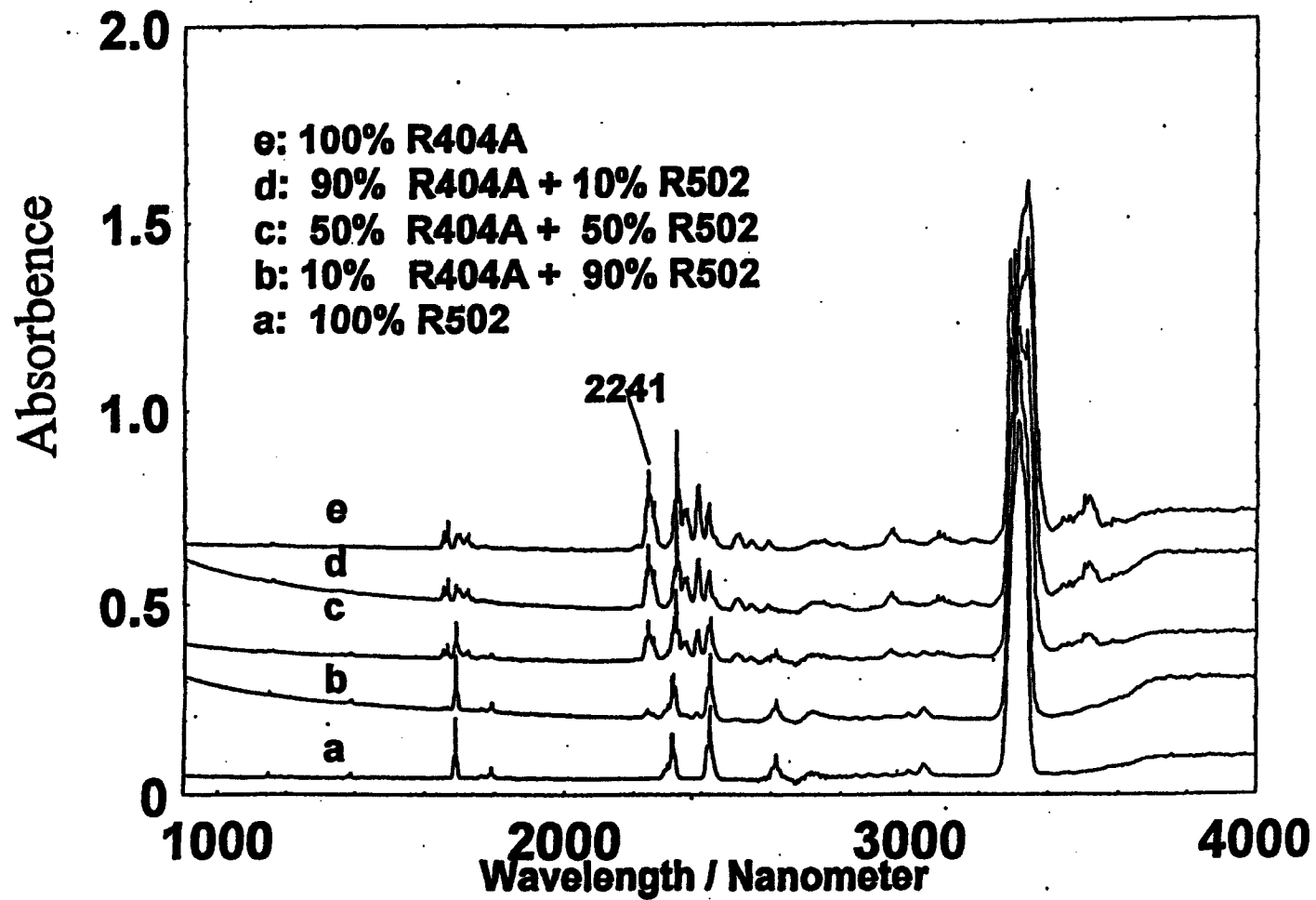


Figure 20. Absorption of different percentages of R-404A and R-502